Quantum Monte Carlo formulation of volume polarization in dielectric continuum theory

Claudio Amovilli,[1,a)] Claudia Filippi,[2] and Franca Maria Floris[1]
[1]*Dipartimento di Chimica e Chimica Industriale, Università di Pisa, Via Risorgimento 35, 56126 Pisa, Italy*
[2]*Instituut-Lorentz, Universiteit Leiden, P.O. Box 9506, NL-2300 RA Leiden, The Netherlands and Faculty of Science and Technology and MESA+ Research Institute, University of Twente, P.O. Box 217, 7500 AE Enschede, The Netherlands*

(Received 25 September 2008; accepted 19 November 2008; published online 29 December 2008)

We present a novel formulation based on quantum Monte Carlo techniques for the treatment of volume polarization due to quantum mechanical penetration of the solute charge density in the solvent domain. The method allows to accurately solve Poisson's equation of the solvation model coupled with the Schrödinger equation for the solute. We demonstrate the performance of the approach on a representative set of solutes in water solvent and give a detailed analysis of the dependence of the volume polarization on the solute cavity and the treatment of electron correlation. © *2008 American Institute of Physics*. [DOI: 10.1063/1.3043804]

I. INTRODUCTION

The dielectric continuum model of solvation is among the most widely used methods in studying the effects of a solvent on the properties of a molecular system.[1–3] Dielectric continuum theory allows one to approximately include the effects of the electrostatic potential produced by the polarization of the solvent in the presence of a solute. These effects are responsible for a significant fraction of the free energy of solvation, namely, the so-called polarization free energy.[1] Even though the polarization free energy is generally not the leading term in the decomposition of the free energy of solvation,[4] it is the most important contribution due to the solvent in processes like chemical reactions[5] and responses to external fields[6] occurring in solution.

Within the dielectric continuum approach, the calculation of the polarization free energy is performed by placing the solute molecule in a cavity created in a dielectric continuum medium representing the solvent. The polarization occurs when we consider the coupling of Poisson's equation of the solute charges (electrons and nuclei) in the dielectric medium, and the Schrödinger equation for the solute electrons in the solvent reaction field.[2,3] All modern packages for standard *ab initio* calculations contain codes to solve more or less rigorously this coupled problem for solutes of arbitrarily complicated shape.[7,8]

Computational difficulties arise when a significant fraction of solute electrons are found in the spatial domain of the solvent, namely, outside the cavity.[9–12] While the shape and size of the cavity are determined based on reasonable physical constraints, the tails of the solute electronic distribution extend in principle to infinity and, especially for anions, charge penetration of the solute in the solvent region cannot be avoided. In the standard polarizable continuum model (PCM),[1] charge penetration is neglected and a charge distribution on the surface of the cavity is determined to yield the solvent dielectric polarization. When charge penetration is considered, the exact solution of Poisson's equation is instead achieved by adding to this surface charge density a volume polarization charge distribution due to the solute in the solvent domain.[11,12] This approach is often referred to as the fully polarized continuum model or the surface and volume polarization for electrostatics (SVPE) method.

In this work, we present an alternative formulation of the SVPE within a quantum Monte Carlo (QMC) framework. In conventional SVPE techniques, the volume polarization charge distribution is represented by a set of point charges placed in the spatial domain of the solvent. The positions of the charges are defined by a grid whose shape can be updated self-consistently. Here, we show how QMC techniques allow a more flexible sampling of these positions which can be modulated on the tail distribution of the solute wave function. The accuracy of the method is demonstrated on a set of prototypical solute molecules in water solution at ambient condition. Our results also indicate that electron correlation tends to reduce the solvent polarization and that the volume polarization has a non-negligible effect on the solute wave function.

This paper is organized as follows. In Sec. II, we describe the proposed approach focusing on its novel features. In Sec. III, we present accurate calculations on a variety of molecules in water solvent. We also investigate the behavior of the polarization free energy contribution with the size of the cavity. In Sec. IV, we draw the conclusions and discuss future prospects.

II. THEORY

When the nuclei and the electrons of a solute are placed within a cavity in a dielectric continuum medium, Poisson's equation takes the form

[a)]Electronic mail: amovilli@dcci.unipi.it.

$$\text{div}\,\mathbf{E} = 4\pi\rho^{(\text{tot})}, \tag{1}$$

where $\mathbf{E}$ is the total electric field and $\rho^{(\text{tot})}$ is the total charge density given by the nuclear and electronic distribution of the solute, and the polarization charge distribution due to the response of the medium to the presence of the solute. The polarization charge density contains two contributions, one coming from the surface of the cavity where the dielectric constant is discontinuous and one from the solvent regions where the dielectric constant is different from the vacuum value and the probability of finding an electron of the solute is not negligible.

A. Volume polarization charge density

We begin with the calculation of the second contribution to the polarization charge density, namely, the so-called volume polarization charge density, given by

$$\rho_{\text{vol}}^{(\text{pol})}(\mathbf{r}) = \left(\frac{1}{\epsilon} - 1\right)\rho_e(\mathbf{r}), \tag{2}$$

where $\rho_e(\mathbf{r})$, in a.u., is the electronic density defined as

$$\rho_e(\mathbf{r}) = -\langle\Psi|\sum_{i=1}^{N}\delta(\mathbf{r}-\mathbf{r}_i)|\Psi\rangle, \tag{3}$$

with N the number of electrons and Ψ the solute wave function.

$\rho_{\text{vol}}^{(\text{pol})}(\mathbf{r})$ is nonzero only outside the cavity where the dielectric constant of the solvent is different from 1. The contribution to the electrostatic potential due to the volume polarization charge density is given by the following integral over the domain outside the cavity $\mathcal{C}$:

$$\begin{aligned}\phi_{\text{vol}}^{(\text{pol})}(\mathbf{r}) &= \int_{\mathbf{r}'\notin\mathcal{C}}\frac{\rho_{\text{vol}}^{(\text{pol})}(\mathbf{r}')}{|\mathbf{r}-\mathbf{r}'|}d\mathbf{r}' \\ &= \left(1-\frac{1}{\epsilon}\right)\langle\Psi|\sum_{i=1}^{N}\frac{\theta(\mathbf{r}_i)}{|\mathbf{r}-\mathbf{r}_i|}|\Psi\rangle,\end{aligned} \tag{4}$$

where $\theta(\mathbf{r})$ is equal to 1 outside and to 0 inside the cavity. As we explain in detail below, we adopt the commonly used definition of a cavity in terms of interlocking spheres. Consequently, a given point is considered outside the cavity if the distance of the point from the center of each sphere is greater than the corresponding radius.

In the variational Monte Carlo (VMC) approach, the integral [Eq. (4)] can be easily estimated by sampling a set of configurations $(\mathbf{r}_1^{(k)},\ldots,\mathbf{r}_N^{(k)})$ from the square of the wave function Ψ^2 using the Metropolis Monte Carlo method. The values of the integrand computed with these configurations are averaged to give

$$\phi_{\text{vol}}^{(\text{pol})}(\mathbf{r}) \approx \frac{1}{M}\sum_{k=1}^{M}\left[\left(1-\frac{1}{\epsilon}\right)\sum_{i=1}^{N}\frac{\theta(\mathbf{r}_i^{(k)})}{|\mathbf{r}-\mathbf{r}_i^{(k)}|}\right], \tag{5}$$

where the estimate tends to the exact result as $M\to\infty$. If we compare this expression with the analogous equation for a discretized set of n_c volume polarization charges:

$$\phi_{\text{vol}}^{(\text{pol})}(\mathbf{r}) \approx \sum_{l=1}^{n_c}\frac{q_l}{|\mathbf{r}-\mathbf{r}_l|}, \tag{6}$$

we see that our expression corresponds to $n_c \leq N\times M$ point charges with charge $q_l=(1-1/\epsilon)/M$ and positions $\mathbf{r}_l=\mathbf{r}_i^{(k)}$ if $\theta(\mathbf{r}_i^{(k)})=1$, corresponding to the sampled one-electron coordinates outside the cavity.

B. Surface polarization charge

For the computation of the polarization charge at the cavity surface, we slightly modify the traditional scheme. Once the electric field has been obtained after some self-consistent procedure, the surface polarization charge density σ at the position $\mathbf{r}$ of the cavity border is given by the relation

$$\sigma(\mathbf{r}) = \frac{(1-\epsilon)}{4\pi\epsilon}\mathbf{n}_+\cdot\mathbf{E}_-(\mathbf{r}), \tag{7}$$

where $\mathbf{n}_+$ is the unity vector pointing from $\mathbf{r}$ outside the cavity and $\mathbf{E}_-$ is the total electric field evaluated at the surface immediately inside the cavity. The electric field results from the superposition of the fields generated by polarization and free charges and can be written as

$$\mathbf{E} = \mathbf{E}_{\text{solute}} + \mathbf{E}_{\text{surf}} + \mathbf{E}_{\text{vol}}. \tag{8}$$

Using Eqs. (3)–(6), we easily obtain

$$\begin{aligned}&\mathbf{E}_{\text{solute}}(\mathbf{r}) + \mathbf{E}_{\text{vol}}(\mathbf{r}) \\ &\quad\approx \sum_{\alpha}^{\text{nuclei}} Z_\alpha\frac{(\mathbf{r}-\mathbf{R}_\alpha)}{|\mathbf{r}-\mathbf{R}_\alpha|^3} \\ &\quad\quad + \frac{1}{M}\sum_{k=1}^{M}\sum_{i=1}^{N}\left[-1+\theta(\mathbf{r}_i^{(k)})\left(1-\frac{1}{\epsilon}\right)\right]\frac{(\mathbf{r}-\mathbf{r}_i^{(k)})}{|\mathbf{r}-\mathbf{r}_i^{(k)}|^3},\end{aligned} \tag{9}$$

where $\mathbf{R}_\alpha$ is the vector position of the solute nucleus α. This equation is formally exact only in the limit of $M\to\infty$ but, for the VMC calculations presented in this paper, the length of the run can be easily made sufficiently long to ensure a small statistical error.

For the surface charge contribution, we have instead

$$\mathbf{n}_+\cdot\mathbf{E}_{\text{surf}-}(\mathbf{r}) = -2\pi\sigma(\mathbf{r}) + \int_\Sigma\frac{\mathbf{n}_+\cdot(\mathbf{r}-\mathbf{r}_a)}{|\mathbf{r}-\mathbf{r}_a|^3}\sigma(\mathbf{r}_a)da, \tag{10}$$

where the integral is defined over the cavity surface Σ. As in standard PCM, the cavity is here defined as the outermost surface obtained by centering spheres of different radii on the solute nuclei. The surface charge distribution σ is discretized by dividing the surface in small area elements and placing point charges at the center of each of them. While, in standard PCM, such elements have well defined shapes, we adopt here a different approach. First of all, we fix the number of point charges per unit surface, p, say, which is chosen to be the same on all the spheres of the cavity. When not too close to a seam between two spheres, a point charge is assigned to a portion of surface with area a given by the inverse of the number density p. The surface charge density σ

at the position $\mathbf{r}_k$ of the point charge q_k is thus approximated as

$$\sigma(\mathbf{r}_k) \approx \frac{q_k}{a}. \tag{11}$$

At the seams where two point charges of different spheres are closer than a fixed length proportional to $\sqrt{a}$, the two point charges are replaced by a single one in the middle, and all properties related to them are averaged with the same weights. An indirect effect of such correction is a smoothening of the cavity surface at the junction between two spheres. In any case, we recall that, since the seams determine a one-dimensional domain, this correction does not significantly alter the value of the surface integral defined above.

The coordinates of the point charges are separately determined on each sphere before these are joined to model the cavity. For a sphere of radius R, the positions of the n point charges ($n=4\pi R^2 p$) are obtained by minimizing the quantity

$$U_n = R\sum_{i=1}^{n-1}\sum_{j=i+1}^{n}\frac{1}{|\mathbf{r}_i - \mathbf{r}_j|}, \tag{12}$$

which does not depend on the radius R. This procedure is equivalent to minimize the repulsion energy between n equal charges constrained on a spherical surface. At the optimal configuration of the n charges, this quantity is a function only of n, namely,

$$U_n = A_n n^2, \tag{13}$$

where A_n equals the series

$$A_n = \sum_{j=0}^{\infty} c_j n^{-j/2} = \frac{1}{2} - \frac{0.552\,47}{\sqrt{n}} + \cdots. \tag{14}$$

This problem is known as the Thomson problem and can be solved by numerical simulations which find the optimal configuration by analyzing the energy of randomly generated configurations from a uniform distribution.[13,14]

Since $2A_n$ is the ratio between the interaction energy of the optimally spaced point charges on a sphere surface and the self-energy of a homogeneous surface distribution of the same total charge, $2A_n$ can be used to correct the surface integral of Eq. (10) where the value is obtained by a summation over a finite set of points. In particular, we adopt the approximation

$$\int_{\Sigma}\frac{\mathbf{n}_+\cdot(\mathbf{r}_k-\mathbf{r}_a)}{|\mathbf{r}_k-\mathbf{r}_a|^3}\sigma(\mathbf{r}_a)da \approx \sum_{j\neq k}\frac{q_j}{2A_{n_j}(j)}\frac{\mathbf{n}_+\cdot(\mathbf{r}_k-\mathbf{r}_j)}{|\mathbf{r}_k-\mathbf{r}_j|^3}. \tag{15}$$

The quantity $A_{n_j}(j)$ is locally defined as

$$A_{n_j}(j) = \frac{R_j}{2n}\sum_{k\neq j}^{\text{sphere}(j)}\frac{1}{|\mathbf{r}_k-\mathbf{r}_j|}, \tag{16}$$

where the sum is restricted to the points generated on the sphere where the charge j lies and also includes those points which will be discarded in forming the solute cavity surface.

This approach does not produce significant differences with the curvature correction used in standard PCM but it allows the use of an arbitrary number of point charges without any reference to surface elements of particular shape. Finally, since the integral (15) and the surface density σ at the point charge positions are linear in q_k, the values of the surface point charges can be obtained by solving the linear system derived from Eq. (7),

$$q_k = \sum_j G_{kj}(\Sigma,\epsilon)\mathbf{n}_+\cdot[\mathbf{E}_{\text{vol}}(\mathbf{r}_j)+\mathbf{E}_{\text{solute}}(\mathbf{r}_j)], \tag{17}$$

where G_{kj} depends only on the shape of the cavity and on the solvent dielectric constant. Equation (17) establishes a relation between Poisson's equation and the solute Schrödinger equation from which the electron density (and subsequently the volume polarization charges) is derived, and is the basis for a self-consistent procedure which leads to a simultaneous solution of both equations.

C. Quantum mechanical treatment of the solute

As many-body wave function to describe the solute, we employ a spin-free Slater–Jastrow form of the type

$$\Psi(\mathbf{r}_1,\mathbf{r}_2,\ldots) = \Phi(\mathbf{r}_1,\mathbf{r}_2,\ldots)\mathcal{J}(r_1,r_2,\ldots,r_{12},\ldots). \tag{18}$$

The determinantal component is given by

$$\Phi = \sum_K D_K^{\uparrow} D_K^{\downarrow} d_K, \tag{19}$$

where $D_K^{\uparrow}$ and $D_K^{\downarrow}$ are the Slater determinants constructed from the occupied orbitals of spin-up and spin-down electrons, respectively, and d_K are the mixing coefficients. The Jastrow correlation factor $\mathcal{J}$ is the exponential of the sum of three fifth-order polynomials of the electron-nuclear (e-n), the electron-electron (e-e), and of pure three-body mixed e-e and e-n distances, respectively.[15] In this work, we use a single-determinantal wave function for all saturated solutes and a multideterminantal reference for the unsaturated systems. In the latter case, the starting determinantal part is obtained from a complete active space self-consistent field (CASSCF) scheme involving the π electrons and one active orbital for each center of the π fragment.

All determinantal and Jastrow parameters of the solute wave function Ψ are simultaneously optimized within VMC by energy minimization.[16] In particular, the optimization of the wave function parameters is achieved using Eq. (17) together with the minimization of the energy functional

$$F[\Psi] = \langle\Psi|\mathcal{H}_{\text{elec}}|\Psi\rangle + \sum_{\alpha<\beta}\frac{Z_\alpha Z_\beta}{|\mathbf{R}_\alpha-\mathbf{R}_\beta|} + \frac{1}{2}\int\left[\sum_\alpha Z_\alpha\delta(\mathbf{r}-\mathbf{R}_\alpha)+\rho_e(\mathbf{r})\right]\sum_k^{\text{surf,vol}}\frac{q_k}{|\mathbf{r}-\mathbf{r}_k|}d\mathbf{r}, \tag{20}$$

where $\mathcal{H}_{\text{elec}}$ is the Hamiltonian of the solute electrons in the field of the solute nucleus α. The last term in the right hand side of Eq. (20) is a sum over all surface and volume charges and corresponds to the so-called polarization contribution to the free energy of solvation.

The basic loop of self-consistency we adopt is the following: (i) At the jth iteration, a VMC run is performed to

TABLE I. Comparison of HF, UQCISD, VMC, and DMC total energies for the systems treated in this work *in vacuo* and with the basis set described in the text. We also include the root-mean-square fluctuations of the local energy computed in VMC (σ). The statistical error on the VMC and the DMC energies is given in parentheses. Data are in a.u.

System	HF	UQCISD	VMC	σ	DMC
F^-	−23.983 20	−24.194 00	−24.3014(1)	0.537 78	−24.3127(1)
CH_3F	−31.262 91	−31.620 00	−31.7520(2)	0.665 15	−31.7825(1)
NH_2NH_2	−21.753 96	−22.146 88	−22.2353(2)	0.558 17	−22.2657(1)
CH_3NH_2	−18.157 90	−18.526 81	−18.6079(2)	0.494 31	−18.6347(1)
CN^-	−15.245 56	−15.548 15	−15.6187(2)	0.482 28	−15.6411(2)
C_2H_2	−12.123 10	−12.404 81	−12.4728(1)	0.421 68	−12.4927(2)
HCHO	−22.448 18	−22.795 52	−22.8859(2)	0.568 66	−22.9113(2)
CH_3CHO	−29.150 58	−29.655 04	−29.7782(3)	0.643 92	−29.8172(2)
CH_3CONH_2	−39.498 93	−40.181 54	−40.3534(3)	0.751 97	−40.4053(2)
CH_3COCH_3	−35.849 49	−36.512 62	−36.6715(3)	0.712 41	−36.7204(2)

generate a new set of volume polarization charges $\mathbf{q}^{(j+1)}$ [Eq. (5)] given a previous set $\mathbf{q}^{(j)}$ and the solute wave function $\Psi^{(j)}$; (ii) with the solvent reaction field described by the new set of charges $\mathbf{q}^{(j+1)}$, the optimal wave function $\Psi^{(j+1)}$ is obtained by energy minimization. At convergence, a diffusion Monte Carlo (DMC) calculation can also be performed using the converged polarization charges determined in VMC and the corresponding optimal wave function. The algorithm has been implemented in the CHAMP package.[17]

III. TEST CALCULATIONS

In order to test the approach presented in Sec. II, we compute the polarization free energy for several solutes in water as solvent. We consider the following solute systems of increasing complexity: fluoride anion (F^-), cyanide anion (CN^-), formaldehyde (HCHO), acethylene (C_2H_2), hydrazine (NH_2NH_2), methylamine (CH_3NH_2), methylfluoride (CH_3F), acetaldeyde (CH_3CHO), acetamide (CH_3CONH_2), and acetone (CH_3COCH_3). For these systems, we compute the surface and volume polarization contributions to the free energy of solvation together with the fraction of electrons found outside the cavity for a series of cavity sizes. Although not realistic, the smallest cavities studied in this work allow us to truly assess the performance of our approach since these small sizes correspond to a very strong volume polarization of the solvent. Similar studies have been published by Chipman[11,12] with whom we will also compare our results.

A. Computational details

In this work, we use scalar-relativistic energy-consistent Hartree–Fock (HF) pseudopotentials[18] which are well designed for QMC calculations. Apart from fluorine which is treated as explained below, we employ the Gaussian cc-pVDZ basis sets[18] constructed for these pseudopotentials and augment them with diffuse functions to ensure a better description of the tails of the wave functions. In particular, we add a diffuse *s* and, for the heavy atoms, also a diffuse *p* Gaussian function with exponents which are a third of the most diffuse single-Gaussian *s* and *p* basis functions of the cc-pVDZ set. For the fluoride anion, in order to improve the representation of the charge density, we modified the cc-pVDZ basis set[18] by discarding the single-Gaussian *s* and *p* basis functions and by decontracting the two most diffuse primitive Gaussians from the original *s* and *p* contracted basis functions. For instance, if we consider the *s* channel, the original *s* contracted basis function is built from nine primitive Gaussians and is now decontracted in 3*s* basis functions, i.e., two single-Gaussian functions with the most diffuse ex-

TABLE II. Surface (ΔG_{surf}), volume (ΔG_{vol}), and total (ΔG_{pol}) polarization contributions to the free energy of solvation for the fluoride anion in water and different cavity radii (R). We list the total polarization computed using (a) our approach and (b) the formula given in Ref. 20 (in the linear regime and for hard-sphere cavity) computed with the same VMC electron density as in (a). q_{out} is the fractional number of solute electrons outside the cavity. Radii are in bohr and polarization energies are in kcal/mol.

R	q_{out}	ΔG_{surf}	ΔG_{vol}	ΔG_{pol}(a)	ΔG_{pol}(b)
1.54	1.961	92.66(4)	−212.15(4)	−119.49(4)	−119.42
1.70	1.536	60.65(3)	−169.74(4)	−109.09(4)	−109.08
2.00	0.987	−1.442(1)	−105.706(4)	−107.148(4)	−107.22
2.20	0.750	−29.335(2)	−76.706(4)	−106.041(4)	−106.25
2.40	0.572	−49.004(1)	−55.619(1)	−104.623(1)	−104.63
2.60	0.437	−61.495(2)	−40.390(1)	−101.885(2)	−102.01
2.80	0.337	−68.732(4)	−29.67(1)	−98.40(1)	−98.36
3.00	0.264	−72.409(1)	−22.005(2)	−94.414(2)	−94.42
3.60	0.129	−73.335(1)	−9.300(1)	−82.635(1)	−82.79
4.00	0.082	−70.194(1)	−5.374(1)	−75.569(1)	−75.64

ponents and one contracted basis function constructed from the remaining seven Gaussian functions without changing the original coefficients. In addition, we add two *s* and two *p* diffuse functions with exponents in the same geometrical sequence of the two decontracted Gaussians.[19] For all systems, we use the equilibrium geometries *in vacuo* obtained in an all-electron unrestricted quadratic configuration interaction with single and double excitations (UQCISD) calculation with the 6-311++G** basis set implemented on the GAUSSIAN 03 package.[8]

In Table I, we list the energies calculated *in vacuo* for all the systems using the HF, the UQCISD, the VMC, and the DMC approaches. We note that the quality of the VMC wave functions is rather good as VMC recovers more than 94% of the DMC correlation energies while UQCISD only recovers between 65% and 75%.

For the relative dielectric constant of water, we use the value of 78.4 at 298 K. To compute the surface polarization contribution, we use a surface number density of point charges equal to $p=1.831$ a.u.$^{-2}$ and a cutoff distance of 0.562 a.u. for averaging at the seams between two interlocking spheres. The number of volume point charges depends on the escaped charge, and the MC runs are taken sufficiently long to guarantee at least 60 000 point charges per escaped electron.

B. Fluoride anion

The treatment of the fluoride anion is simple since, for a given electronic density, the polarization contribution to the free energy of solvation can be computed exactly. Therefore, to assess the quality of the discretization of the solvent polarization charge distribution used in our approach, we start from the converged electronic density computed according to the self-consistent scheme presented in Sec. II and solve this part of the calculation exactly. For the exact computation of the polarization free energy, we follow the approach we recently published on nonlinear solvent polarization for spherical solutes,[20] which we here consider of course in the limit of linearity and for a hard-sphere cavity.

In Table II, we list the VMC polarization free energies computed for different cavity radii at self-consistency and compare them with the values calculated exactly starting from the same, final VMC density. Although the differences between the two sets of values are greater than the statistical error, the discrepancies always remain below 0.2 kcal/mol. Therefore, considering that the variation in polarization energy over the range of the considered cavity radii is about 200 times greater, we can regard the numerical error associated with the discretization of the charge as small and the approximation as sufficiently accurate.

Furthermore, we compare our approach with one of the most commonly used PCM methods, that is, the so-called integral equation formalism (IEF) PCM (Ref. 9) in the version implemented in the GAUSSIAN package.[8] In the standard IEF-PCM approach, the volume polarization charge is simulated via an effective surface polarization which produces the same effect inside the cavity. For the quantum mechanical treatment of the solute in these IEF-PCM calculations, we use the density functional theory (DFT) with the B3LYP exchange-correlation functional and employ the same pseudopotentials and basis sets as in the QMC calculations.

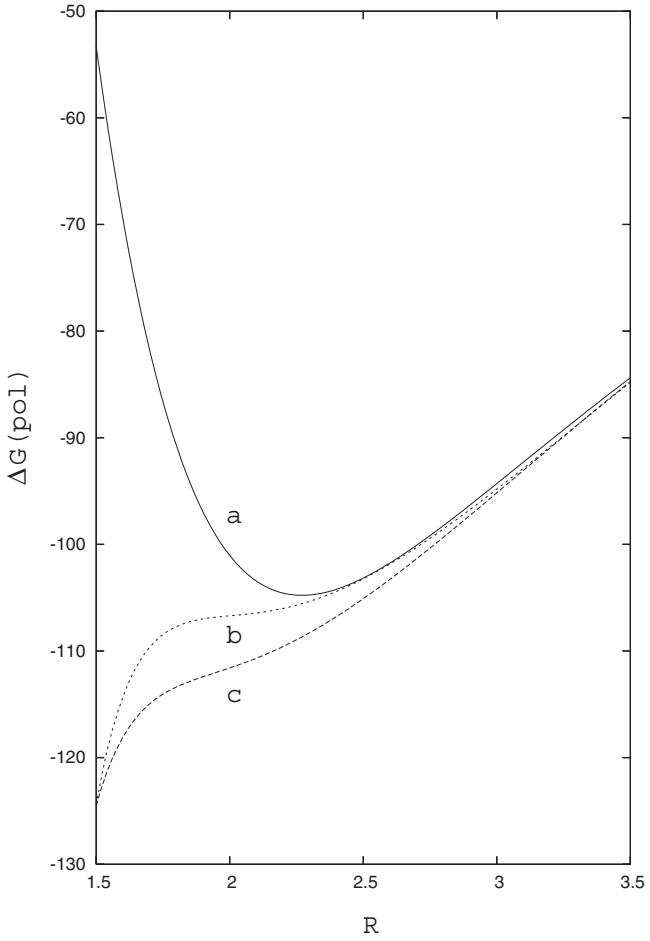

FIG. 1. Polarization contribution to the free energy of solvation of the fluoride anion in water solution as a function of the cavity radius. Curve a refers to the IEF-PCM method, curve b to this work, and curve c to the solution of Poisson's equation with the IEF-PCM fluorine electron density. Energies are in kcal/mol and radii are in bohr.

The polarization energies computed with our method and with the IEF-PCM/DFT-B3LYP approach are shown in Fig. 1 as a function of the cavity radius. Our QMC results (curve b) only suffer from the numerical error coming from the discretization of the polarization charge distribution discussed above, which is not visible on the scale of the plot. On the other hand, as already noted by Chipman,[12] the IEF-PCM approximate treatment of volume polarization (curve a) leads to an incorrect behavior for small cavity radii while it tends to the exact result at larger radii. It is important to stress that the standard PCM without any treatment of the volume polarization would lead to significantly worse results. Finally, we also compute the exact polarization energy using the electron density resulting from the Gaussian IEF-PCM calculation (curve c). Although curve c is more accurate than curve a computed with the IEF-PCM approximate treatment of volume polarization, the discrepancies for small cavities indicate that, when the solvent reaction field is strong, the sensitivity of the solute electronic response to the

solvent polarization can be significant leading to not negligible errors if the solvent polarization itself is not properly described.

For completeness as we do for the other solutes, in Table II, we also show the surface and the volume polarization contribution together with the fractional number of fluorine electrons falling outside the cavity. If we look at the separate volume and surface contributions, it is interesting to note the large variation in the volume polarization with the change in the cavity radius and the change in sign of the surface polarization term when there is one escaped electron.

C. Two heavy atom solutes (N_2H_4, CH_3NH_2, CN^-, C_2H_2, HCHO, and CH_3F)

Here, we consider the solutes which contain two heavy (not hydrogen) atoms. In order to analyze the polarization free energy term for cavities of different sizes, we have varied the radii of the spheres according to a rule which depends on only one cavity size parameter. For a given molecule X, once the radius of a sphere centered on atom j has been fixed, the radii R_i^X for all other centers are derived from the relation

$$R_i^X = a_{ij}^X + b_{ij}^X R_j^X, \tag{21}$$

where a_{ij}^X and b_{ij}^X are constant parameters. These parameters are computed by fitting the resulting surface to the two-dimensional isodensity contours obtained by a standard DFT-B3LYP calculation performed *in vacuo* at the equilibrium geometry. For each system, we consider several cavities and determine one set of optimal fitting parameters, a_{ij}^X and b_{ij}^X, for all radii.

In Table III, we report the surface (ΔG_{surf}), the volume (ΔG_{vol}), and the total (ΔG_{pol}) polarization contribution to the free energy of solvation computed in our VMC scheme for different cavity radii. We compare our QMC results with the polarization free energies computed with the same basis set and pseudopotentials and the IEF-PCM approach in GAUSSIAN 03 at the restricted HF ($\Delta G_{\text{pol}}^{\text{RHF}}$) and the DFT ($\Delta G_{\text{pol}}^{\text{DFT}}$) level of theory. Finally, in Table IV, we give all the parameters which define the solute cavity in our calculations.

The cavities we consider vary from a size roughly corresponding to a contact with the solute (the fractional amount of electrons outside the cavity, q_{out}, is small) to a size where one solute electron is outside the cavity. To estimate the radii typically used in standard PCM calculations, we can consider the Bondi radii[21] multiplied by 1.2, as it has been done for a long time in the past, and find 3.52, 3.86, 3.45, and 3.33 bohr for N, C, O, and F, respectively. These values are close to our largest radii and indicate that, in standard PCM applications, a fraction of solute electrons, ranging between 0.1 and 0.2, falls outside the cavity in the solvent domain. From our VMC calculations for all neutral systems, we see that an escaped charge of similar magnitude yields a volume polarization contribution which is very small in comparison to the total polarization term. For the cyanide anion, on the other hand, the volume term is significantly larger and amounts to roughly 10%–15% of the total polarization energy. It is also interesting to notice that the sign of ΔG_{vol} for small cavities is positive for the neutral solutes and negative for the anion. Therefore, in the neutral case, the interaction of the positive volume polarization charges with the nuclei is dominant while, in the anionic case, the interaction with the electrons is more important because the number of electrons is greater than the total nuclear charge.

The results obtained with our VMC scheme and the DFT-B3LYP energies computed with the IEF-PCM method allow us to understand the effect of electron correlation on the polarization contribution to the energy of solvation. If we compare the HF and DFT-B3LYP polarization energies of Table III, we observe that correlation tends to reduce in modulus the polarization free energy for all studied systems and all cavity radii. For the largest cavity radii where a comparison of our approach and the IEF-PCM is meaningful, we also find that the DFT-B3LYP polarization energies obtained with the IEF-PCM agree well with the VMC results but are always slightly higher in modulus than the VMC values. This further indicates that a better treatment of correlation as the one obtained in VMC has the effect of reducing the polarization free energies.

For these small-sized systems, the description of the electronic density in DFT-B3LYP appears to be sufficiently accurate to give a reasonable estimate of the polarization free energy. The favorable comparison of the DFT-B3LYP energies with the VMC values at large cavity radii supports the adequacy of DFT. Even for the cyanide anion where the polarization is strong, the DFT-B3LYP energies compare well with the results of a CASSCF calculation within the IEF-PCM. As shown in Fig. 2, the DFT-B3LYP polarization energies of the cyanide anion are very close to the results of a CAS(10,10) calculation (all ten valence electrons are placed in ten active orbitals) over the whole range of escaped charge. We remark that we perform CASSCF instead of coupled cluster or extensive configuration interaction calculations because the GAUSSIAN 03 package computes the dielectric polarization charges self-consistently only at the HF, DFT, and CASSCF levels while leaving the charges at the values determined for the one-determinant reference wave function in all other cases.

For the smallest cavities, the comparison of our VMC results with the HF or DFT energies computed with the IEF-PCM is not meaningful, as we have seen in the case of the fluoride anion. However, we can compare our VMC energies with the accurate solution of Poisson's equation at the HF level obtained by Chipman[12] for the cyanide anion. Since the cavities in Chipman's work are constructed in a slightly different way, a comparison is possible only by plotting the energies as a function of the escaped charge as done in Fig. 2. Our VMC and Chipman's curves, also shown in Fig. 2, are not too dissimilar in shape and the difference in magnitude must be mainly ascribed to electron correlation. This difference is similar to the difference between the IEF-PCM

TABLE III. Solute cavity data (see text) and calculated polarization free energy for the two-heavy-center solutes in water considered in this work. Our results are compared with the IEF-PCM energies obtained from GAUSSIAN 03 at the RHF and DFT-B3LYP levels. Radii and charges are in a.u. and free energy contributions are in kcal/mol.

R_j^X	q_{out}	ΔG_{surf}	ΔG_{vol}	ΔG_{pol}	ΔG_{pol}^{RHF}	ΔG_{pol}^{DFT}
			j=N X=N_2H_4			
3.921	0.099	−4.853(4)	−0.1106(1)	−4.964(4)	−6.16	−5.88
3.647	0.155	−6.305(6)	−0.1446(3)	−6.45(6)	−8.15	−7.76
3.269	0.291	−9.90(1)	−0.180(1)	−10.08(1)	−12.51	−11.87
2.948	0.499	−15.43(1)	0.108(2)	−15.32(1)	−18.78	−17.76
2.702	0.751	−20.80(1)	1.706(3)	−19.09(1)	−26.65	−25.24
2.324	1.422	−50.32(2)	9.51(1)	−40.81(3)	−49.62	−47.53
			j=C X=CH_3NH_2			
4.082	0.089	−2.484(4)	−0.0326(1)	−2.516(4)	−3.11	−2.97
3.685	0.173	−3.825(5)	−0.0294(3)	−3.855(5)	−4.66	−4.44
3.364	0.295	−5.722(7)	0.0526(7)	−5.670(7)	−6.71	−6.38
3.024	0.522	−9.87(2)	0.563(4)	−9.31(2)	−10.36	−9.82
2.646	0.984	−21.78(1)	3.264(4)	−18.52(1)	−18.20	−17.37
2.343	1.630	−49.69(3)	11.83(2)	−37.86(4)	−32.05	−31.07
			j=C X=CN^-			
4.535	0.100	−55.141(1)	−5.5690(2)	−60.710(1)	−62.05	−61.33
4.120	0.166	−54.952(2)	−9.8253(3)	−64.778(2)	−66.41	−65.40
3.628	0.311	−49.396(3)	−20.0746(8)	−69.471(3)	−71.52	−70.09
3.099	0.566	−33.848(3)	−40.188(2)	−74.037(3)	−75.62	−73.69
2.797	0.822	−14.030(3)	−61.287(3)	−75.317(5)	−75.79	−73.56
2.457	1.264	21.270(6)	−97.631(7)	−76.36(1)	−71.86	−69.16
			j=C X=C_2H_2			
4.120	0.083	−2.325(3)	−0.0803(1)	−2.405(3)	−3.18	−2.67
3.742	0.151	−3.009(4)	−0.1108(3)	−3.120(5)	−4.62	−3.90
3.383	0.268	−4.575(5)	−0.0967(7)	−4.672(5)	−6.86	−5.85
3.024	0.476	−8.480(7)	0.110(2)	−8.370(7)	−10.54	−9.20
2.721	0.770	−15.451(9)	1.413(4)	−14.04(1)	−15.83	−14.16
2.362	1.353	−38.98(2)	8.42(1)	−30.56(2)	−28.55	−26.60
			j=O X=HCHO			
3.638	0.077	−3.615(5)	0.0062(1)	−3.609(5)	−6.23	−4.54
3.345	0.136	−4.841(6)	0.0867(2)	−4.755(6)	−8.43	−6.16
3.024	0.254	−7.221(8)	0.3723(6)	−6.849(9)	−12.36	−9.08
2.731	0.451	−11.24(1)	1.441(1)	−9.80(1)	−18.32	−13.56
2.447	0.783	−21.25(2)	4.804(4)	−16.45(2)	−30.14	−22.70
2.183	1.312	−48.87(2)	15.056(9)	−33.82(3)	−50.84	−39.89
			j=F X=CH_3F			
3.345	0.084	−2.371(5)	0.0118(1)	−2.360(5)	−3.42	−2.94
3.118	0.140	−3.081(6)	0.0759(2)	−3.005(6)	−4.31	−3.72
2.872	0.243	−4.371(7)	0.3108(6)	−4.061(7)	−5.76	−4.99
2.608	0.437	−7.48(1)	1.177(2)	−6.31(1)	−8.36	−7.33
2.400	0.693	−13.20(1)	3.224(3)	−9.98(1)	−12.08	−10.76
2.117	1.287	−37.59(2)	12.53(1)	−25.05(3)	−23.29	−21.51

curves obtained at the HF and the DFT-B3LYP correlated level. More recently, Chipman[11] also separately analyzed the volume and surface polarization terms within HF for one cavity size with q_{out}=0.17. From Table III, we find that the ratio $\Delta G_{vol}/\Delta G_{surf}$ at q_{out}=0.166 is 0.179, which is in agreement with Chipman's ratio of 0.182.[11] Therefore, correlation lowers both surface and volume polarization contributions by equal amounts.

While Table III illustrates how the effect of electron correlation is similar in DFT and VMC, it is nevertheless important to note that the DFT and VMC data do not go to the same limit at large cavities. The difference in the limiting polarization free energies varies from 0.26 kcal/mol for C_2H_2 to 0.93 kcal/mol for HCHO. This discrepancy increases with the size of the solute as we will explain below where larger systems are considered.

TABLE IV. Parameters used to compute the radii of the cavity spheres as given by Eq. (21). $a_{ij}^{(X)}$ is in bohrs.

System (X)	Center type (i)	$a_{ij}^{(X)}$	$b_{ij}^{(X)}$	Reference (j)
NH_2NH_2	H	−0.749	0.91	N
CH_3NH_2	C_a	0.208	0.95	N
	H_a	−0.737	0.922	N
	H_b	−0.680	0.86	N
CN^-	N	0.227	0.88	C
C_2H_2	H	−0.586	0.81	C
HCHO	H	−0.926	1.07	O
	C	−0.227	1.09	O
CH_3F	H	−1.191	1.22	F
	C	−0.208	1.20	F
CH_3CHO	C_c	0	1.13	O
	H_c	−0.964	1.08	O
	C_a	−0.113	1.13	O
	H_a	−0.850	1.03	O
CH_3CONH_2	C_c	−0.128	1.093	O
	N_b	0.374	0.961	O
	H_b	−0.620	0.881	O
	C_a	0.217	1.046	O
	H_a	−0.794	1.018	O
CH_3COCH_3	C_c	0	1.11	O
	C_a	0	1.10	O
	H_a	−0.794	1.009	O

a-CH_3, b-NH_2, c-C(H)O

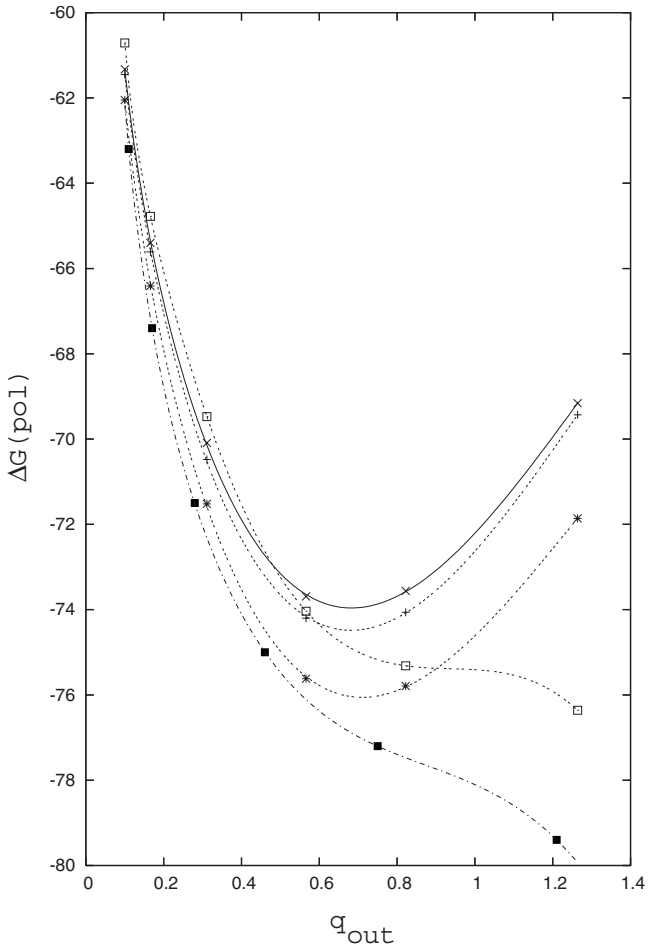

FIG. 2. Polarization contribution to the free energy of solvation of the cyanide anion in water solution as a function of the solute electronic charge outside the cavity from this work (square), from IEF-PCM at the RHF (asterisk), the CAS (10,10) (plus), and the DFT (cross) levels, and from Ref. 12 (filled square). Energies are in kcal/mol and charges are in a.u.

D. Medium size solutes (CH_3CHO, CH_3CONH_2, and CH_3COCH_3)

Common features of acetaldeyde, acetamide, and acetone are that they have three or more heavy atoms and are unsaturated owing to the presence of a carbonyl group. The QMC calculations on these solutes performed with a multideterminantal wave function and a three-body Jastrow correlation factor become computationally much more expensive. Therefore, we limit the calculations to fewer cavity sizes than for the other molecules. All the data are collected in Table V.

The effect of electron correlation in reducing the overall polarization contribution to the solvation energy is here significant. This is evident if we compare our VMC results with the IEF-PCM energies obtained at the RHF level for the largest cavities and, for acetamide, with the HF data at different cavities by Chipman.[12] The comparison with Chipman's results is shown in Fig. 3 where ΔG_{pol} is plotted as a function of the escaped charge. We also observe that the difference between the DFT-B3LYP and the VMC energies for the largest cavities is now significantly larger than for the smaller molecules and amounts to as much as 3 kcal/mol for acetamide.

It is important to remark that the effect of correlation on the solvation in the PCM is not limited to the polarization contribution because the solute wave function will change in the presence of a polarized solvent leading to a change in the solute internal energy. If we denote with $\hat{H}_0$ the solute Hamiltonian and with $V_s/2$ the perturbation due to the polarized dielectric, the polarization contribution to the free energy of solvation is

$$\Delta G_{\mathrm{pol}} = -\langle\Psi|\frac{1}{2}V_s|\Psi\rangle + \frac{1}{2}\sum_{\alpha}\int\frac{Z_\alpha V_s(\mathbf{r})}{|\mathbf{R}_\alpha - \mathbf{r}|}d\mathbf{r}, \tag{22}$$

and the so-called solute internal energy change is given by

$$\Delta G_{\mathrm{iec}} = \langle\Psi|\hat{H}_0|\Psi\rangle - \langle\Psi_0|\hat{H}_0|\Psi_0\rangle, \tag{23}$$

where Ψ and Ψ_0 are, respectively, the solute wave function in solution and *in vacuo*. Because of the variational principle, ΔG_{iec} is always positive. The electrostatic contribution to the solvation free energy is therefore given by

$$\Delta G_{\mathrm{el}} = \Delta G_{\mathrm{pol}} + \Delta G_{\mathrm{iec}}, \tag{24}$$

and, when we minimize the energy of the solute in the dielectric medium [Eq. (20)], we minimize

TABLE V. Solute cavity data (see text) and calculated polarization free energy for the medium-sized solutes in water considered in this work and comparison with IEF-PCM results obtained from GAUSSIAN 03 at the RHF and DFT-B3LYP levels. Radii and charges are in a.u. and free energy contributions are in kcal/mol.

R_j^X	q_{out}	ΔG_{surf}	ΔG_{vol}	ΔG_{pol}	ΔG_{pol}^{RHF}	ΔG_{pol}^{DFT}
			j=O X=CH_3CHO			
3.364	0.181	−5.08(1)	0.1149(6)	−4.96(1)	−8.31	−6.56
3.043	0.338	−7.32(1)	0.441(1)	−6.88(1)	−11.73	−9.24
2.769	0.578	−10.97(2)	1.429(3)	−9.54(2)	−16.39	−12.95
			j=O X=CH_3CONH_2			
3.383	0.228	−9.88(1)	−0.0334(7)	−9.91(1)	−14.51	−12.86
3.043	0.427	−14.28(1)	0.183(1)	−14.09(1)	−20.75	−18.41
2.769	0.702	−20.33(3)	0.753(6)	−19.58(3)	−28.20	−24.97
			j=O X=CH_3COCH_3			
3.402	0.228	−5.52(1)	0.1646(6)	−5.36(1)	−8.71	−7.24

$$F[\Psi] = \langle \Psi_0 | \hat{H}_0 | \Psi_0 \rangle + \Delta G_{el}. \quad (25)$$

Therefore, in this minimization, there is a competition between two effects. On the one hand, ΔG_{pol} tends to lower the total energy while ΔG_{iec} determines a friction to polarization. It is therefore clear that the changes in the wave function are better estimated by the use of flexible correlated functional forms like the ones we use here in our VMC approach. From a pure chemical point of view, one can imagine that a multiconfigurational form like in valence bond theory can account for the relative weights of different structures in different polarization situations much better than the single determinant of the HF theory. In Table VI, the VMC electrostatic contribution to the free energy of solvation of acetamide in water is compared with the corresponding terms from IEF-PCM computed within HF, DFT, and UQCISD. As already mentioned, the UQCISD electrostatic contribution is obtained within GAUSSIAN 03 with the polarization charges determined self-consistently for the reference unrestricted HF function. Because of ΔG_{iec}, the differences between the various sets of data are smaller than when comparing the values of ΔG_{pol}. It is important to remark that the QMC statistical error on ΔG_{iec} is greater than the error on ΔG_{pol} because ΔG_{iec} is obtained as the difference of two much larger numbers.

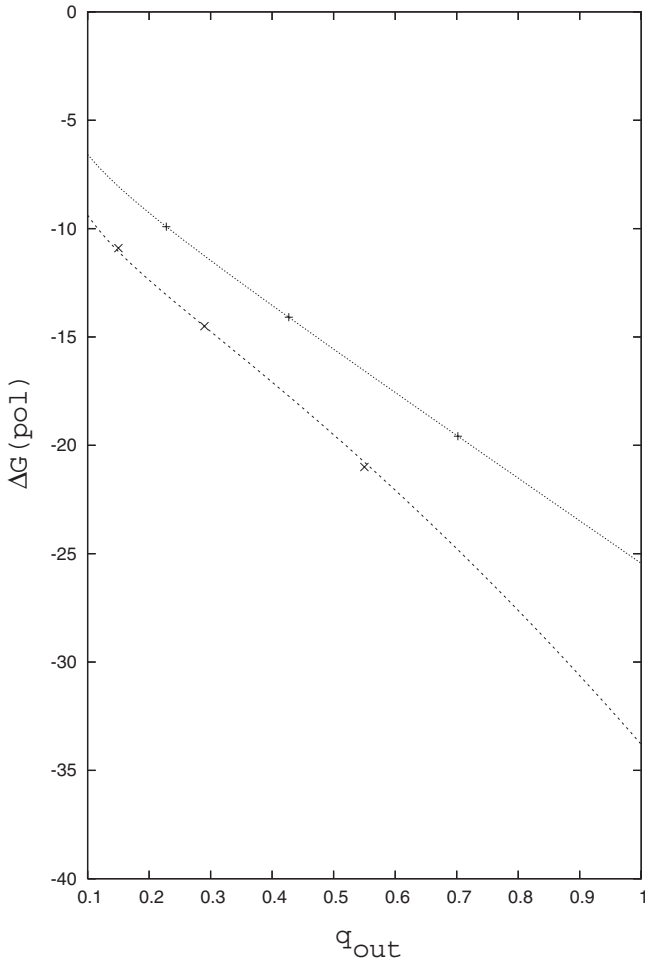

FIG. 3. Polarization contribution to the free energy of solvation of acetamide in water solution as a function of the solute electronic charge outside the cavity from this work (upper curve) and from Ref. 12 (lower curve). Energies are in kcal/mol and charges are in a.u.

For many PCM applications, researchers find HF or DFT plainly satisfactory but here we have shown that, if one allows the method to consider the dielectric polarization and the solute response in a sophisticated manner, the resulting solvation energies can differ substantially in molecules such as acetamide.

Finally, it is interesting to analyze the accuracy of the surface integration. For the fluoride anion, we have shown that this integration is performed almost exactly but, when the symmetry is reduced as in the case of a polyatomic mol-

TABLE VI. Solute cavity data (see text) and electrostatic solvation free energy for acetamide in water calculated with VMC and comparison with IEF-PCM results obtained from GAUSSIAN 03 at the RHF, DFT-B3LYP, and UQCISD levels. Radii are in bohr and free energy contributions are in kcal/mol.

R_j^X	ΔG_{el}^{VMC}	ΔG_{el}^{RHF}	ΔG_{el}^{DFT}	ΔG_{el}^{UQCISD}
		j=O X=CH_3CONH_2		
3.383	−9.1(3)	−11.91	−10.40	−9.84
3.043	−12.9(3)	−16.65	−14.49	−13.83
2.769	−18.8(4)	−22.33	−19.36	−18.60

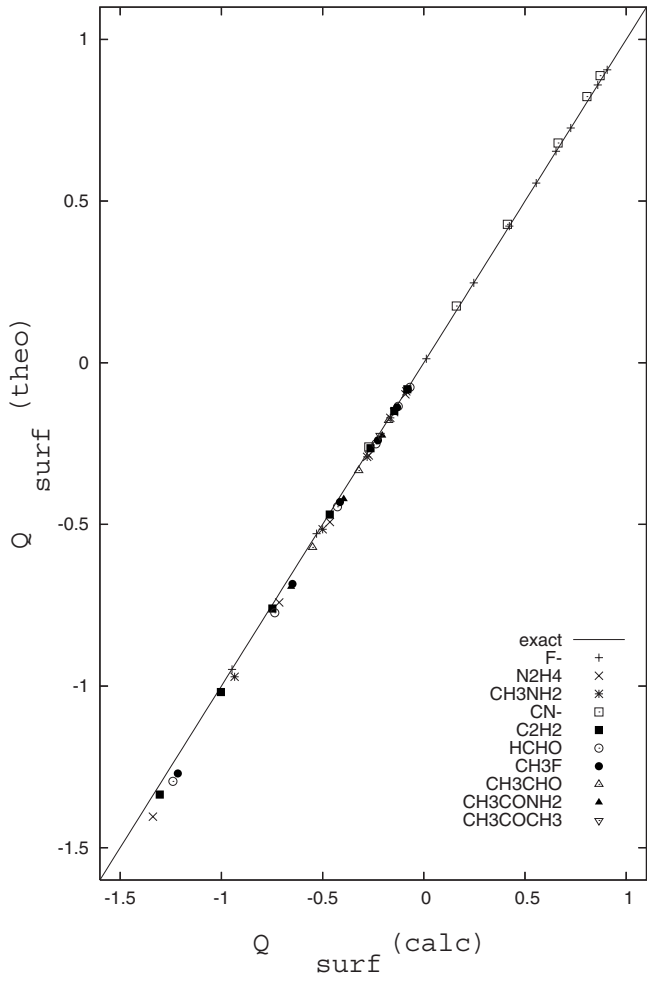

FIG. 4. Theoretical vs calculated total surface polarization charge in a.u.

ecule and the dielectric responds to a nonspherical solute field, we expect in general a larger error. In fact, in such cases, the solvent polarization charges could be both positive and negative and have a rather asymmetrical distribution leading to a much more complicated situation. For the purpose of estimating this error, we compare the total surface polarization charge of the polarized dielectric with the expected theoretical value which can be calculated by using the escaped charge as

$$Q_{\mathrm{surf}} = \left(\frac{1}{\epsilon} - 1\right)(Q_{\mathrm{ion}} + q_{\mathrm{out}}), \tag{26}$$

where Q_{ion} is the charge of the solute (not zero only for ions) and q_{out} is the fractional number of electrons outside the cavity, which is here a positive number as listed in Tables II, III, and V. In Fig. 4, we compare this theoretical value with the surface polarization charge calculated by summing all surface point charges in the VMC calculations for all the molecules and cavity radii. We find that the differences are always smaller than 5% and the largest discrepancies are found for the smallest cavities. These errors in the surface charge integration propagate to ΔG_{surf} and we roughly estimate that the resulting free energy uncertainty is about 5%. By rescaling the surface polarization charge as already done in the past within the PCM,[4,22] one would obtain a more negative value of ΔG_{surf} since the theoretical Q_{surf} is in general more negative than the one calculated by summing all surface point charges. We estimate that a better treatment of the surface charge may reduce the differences with Chipman's HF results by at most 25%. Here, we did not perform any adjustment of the surface polarization charge and will leave this delicate aspect of the model to future work.

TABLE VII. Solute cavity data (see text) and calculated polarization (total and partial) and electrostatic free energies for fluoride anion and formaldehyde at the DMC level. Radii are in bohr and free energy contributions are in kcal/mol.

R_j^X	ΔG_{surf}	ΔG_{vol}	ΔG_{pol}	ΔG_{el}
		j=F X=F$^-$		
1.540	92.60(8)	−211.82(8)	−119.2(1)	−118.9(1)
1.700	60.50(3)	−169.51(4)	−109.01(5)	−108.43(9)
2.000	−1.5018(4)	−105.63(2)	−107.13(2)	−106.5(1)
2.200	−29.349(7)	−76.63(1)	−105.98(2)	−105.40(9)
2.400	−48.90(1)	−55.71(1)	−104.61(1)	−104.2(1)
2.600	−61.46(1)	−40.440(7)	−101.90(1)	−101.6(1)
2.800	−68.71(1)	−29.626(6)	−98.34(1)	−98.2(1)
3.000	−72.424(9)	−22.046(4)	−94.47(1)	−94.46(9)
3.600	−73.368(6)	−9.339(2)	−82.707(7)	−83.1(1)
4.000	−70.184(5)	−5.4660(2)	−75.650(5)	−76.0(1)
		j=O X=HCHO		
3.638	−3.606(4)	0.0017(1)	−3.604(4)	−3.5(1)
3.345	−4.828(6)	0.0882(3)	−4.740(6)	−4.7(1)
3.024	−7.214(9)	0.3884(9)	−6.826(9)	−6.5(1)
2.731	−11.29(1)	1.506(2)	−9.78(1)	−9.4(1)
2.447	−21.30(2)	4.868(5)	−16.43(2)	−16.0(1)
2.183	−48.90(3)	15.03(1)	−33.87(3)	−32.2(1)

E. Diffusion quantum Monte Carlo

Starting from a given trial wave function, the fixed-node DMC method produces the best energy within the fixed-node approximation [i.e., the lowest-energy state with the same zeros (nodes) as the trial wave function]. We slightly modified the DMC code of the CHAMP package in order to explore this opportunity to further improve our results. In the DMC run, we use as trial wave function the one optimized in the dielectric medium with our VMC approach. In the Hamiltonian, we keep the solvent reaction field (surface and volume charges) which has been obtained at convergence in correspondence to the VMC function. We select only F$^-$ and HCHO as solutes for this study and collect the DMC mixed estimators of the polarization energies and the electrostatic component for the different cavities in Table VII.

Despite the large variations in the surface and free energy contributions as a function of the cavity size, the differences with the corresponding energies obtained at the VMC level are always within ±0.1 kcal/mol. Therefore, the Slater–Jastrow forms of solute wave functions we use in this work are sufficiently accurate to properly account for correlation effects in the solution of the PCM problem. From the DMC results, it also appears that the internal energy change contribution is small for these two molecules. We note on the

other hand that, during the VMC optimization in solvent, both polarization and escaped charges changed significantly. This means that the small variation in the internal DMC and VMC energies is due to the great flexibility of our wave function form. The same behavior is, in fact, not observed at a pure RHF level.

In future work, we believe that DMC could be used to accurately compute ΔG_{el} while using much simpler VMC trial wave functions. A consideration which is relevant for large solutes where the use of complex functional forms becomes prohibitive.

IV. CONCLUSIONS

We propose a new formulation of the volume polarization due to solvation of a dielectric medium within the framework of QMC methods. In this approach, the dielectric response is considered in the linear regime and the solute is placed in a cavity made by interlocking spheres centered on the nuclei. The polarization charge density is discretized as a set of point charges positioned on the surface of the cavity and in the region of the dielectric medium where the tail of the solute electron density extends. The surface polarization charges are generated from a uniform distribution while the positions of the volume polarization charges are sampled from the square of the solute wave function. Poisson's equation for the electric field of the solute in a dielectric solvent is then solved self-consistently with the minimization of the solute electronic energy. The solute Hamiltonian includes the solvent reaction field and the wave function chosen here in the Slater–Jastrow form is optimized within a VMC scheme. The main features of the proposed method are (i) the relatively simple and rather accurate treatment of Poisson's equation and (ii) the use of highly correlated wave function forms for the description of the solute electrons.

To validate the method, we have performed numerical tests on selected solutes of different sizes in water solvent at ambient conditions. In order to obtain an enhanced effect of volume polarization, we have also considered unrealistically small cavities as done recently by Chipman[11,12] using the restricted HF method. The results show that electron correlation tends to reduce the solvent polarization and that volume polarization has an effect in changing the solute wave function. Our results for the behavior as a function of cavity size compare qualitatively well with Chipman's work for CN^- and CH_3CONH_2, and the quantitative differences are due to electron correlation and to Chipman's choice of a basis set without diffuse functions.

We have also performed a DMC calculation with the converged VMC solvent reaction field, which yields solvation energy contributions not significantly different from the VMC values. This finding is due to the very accurate form we used for trial wave function which consists of fully optimized sophisticated Jastrow and multideterminantal components. In general, since a rather time-consuming part of the calculation is the computation of the Jastrow factor containing the electron-electron-nucleus three-body terms, one could adopt a simpler wave function form with only a two-body Jastrow factor for large molecular solutes and use the DMC step to improve on the VMC solvation results.

For a given choice of trial wave function, the computational cost of a QMC calculation in solution will roughly be the same as *in vacuo* if the polarization potential is set up and interpolated on a grid. Alternatively, if the polarization potential is computed by summing over all polarization charges, the computational cost will depend on the total number of charges. For example, for CH_3CHO with about 35 000 volume polarization charges, the calculation in solution is about two times as long as *in vacuo*.

Finally, we note that while the volume polarization charges have a simple definition and, in our method, do not suffer from numerical errors in their evaluation, a comparison of the total surface polarization charge obtained in our VMC calculations with the expected value coming from the solute escaped charge showed small differences in some cases. Although such discrepancies are acceptable for practical applications, we think that this point deserves further attention in future work. In particular, one must pay attention to the treatment of Eq. (15) where the surface integral is transformed into a sum over a finite number of points with appropriate weights as in a typical quadrature formula. Here, we used a constant number density of point charges, p, but a better choice could possibly be to introduce different number densities for different spheres. The definition of a more efficient strategy is the subject of further studies.

ACKNOWLEDGMENTS

The authors acknowledge support for computer time from SARA Computing and Networking Services (Amsterdam, The Netherlands) and CINECA High Performing Computing (Bologna, Italy).

[1] S. Miertus, E. Scrocco, and J. Tomasi, Chem. Phys. **55**, 117 (1981).
[2] C. J. Cramer and D. G. Truhlar, Chem. Rev. (Washington, D.C.) **99**, 2161 (1999).
[3] J. Tomasi, B. Mennucci, and R. Cammi, Chem. Rev. (Washington, D.C.) **105**, 2999 (2005).
[4] C. Amovilli, V. Barone, R. Cammi, E. Cances, M. Cossi, B. Mennucci, C. S. Pomelli, and J. Tomasi, Adv. Quantum Chem. **32**, 227 (1999).
[5] C. Amovilli, B. Mennucci, and F. M. Floris, J. Phys. Chem. B **102**, 3023 (1998).
[6] R. Cammi, M. Cossi, B. Mennucci, and J. Tomasi, J. Chem. Phys. **105**, 10556 (1996).
[7] M. W. Schmidt, K. K. Baldridge, J. A. Boatz, S. T. Elbert, M. S. Gordon, J. H. Jensen, S. Koseki, N. Matsunaga, K. A. Nguyen, S. J. Su, T. L. Windus, M. Dupuis, and J. A. Montgomery, J. Comput. Chem. **14**, 1347 (1993).
[8] M. J. Frisch, G. W. Trucks, H. B. Schlegel *et al.*, GAUSSIAN 03, Revision C.02, Gaussian, Inc., Wallingford, CT, 2004.
[9] E. Cances, B. Mennucci, and J. Tomasi, J. Chem. Phys. **107**, 3032 (1997).
[10] D. M. Chipman, J. Chem. Phys. **104**, 3276 (1996).
[11] D. M. Chipman, J. Chem. Phys. **124**, 224111 (2006).
[12] D. M. Chipman, J. Chem. Phys. **116**, 10129 (2002).
[13] C. Amovilli and N. H. March, Chem. Phys. Lett. **347**, 459 (2001).
[14] M. Bowick, A. Cacciuto, D. R. Nelson, and A. Travesset, Phys. Rev. Lett. **89**, 185502 (2002).
[15] C. Filippi and C. J. Umrigar, J. Chem. Phys. **105**, 213 (1996); the electron-electron-nucleus term is modified to contain only pure three-body contributions and the electron-nucleus term is adapted to deal with pseudoatoms. The scaling factor κ is set to 0.5.

[16] C. J. Umrigar, J. Toulouse, C. Filippi, S. Sorella, and R. G. Hennig, Phys. Rev. Lett. **98**, 110201 (2007).
[17] C. J. Umrigar, C. Filippi *et al.*, CHAMP, a quantum Monte Carlo program package, http://www.ilorentz.org/~filippi/champ.html.
[18] M. Burkatzki, C. Filippi, and M. Dolg, J. Chem. Phys. **126**, 234105 (2007).
[19] The four single-Gaussian functions of F have exponents 0.364 875, 0.172 723, 0.081 763, and 0.038 705 for the s shell and 0.204 414, 0.101 001, 0.049 905, and 0.024 658 for the p shell.
[20] C. Amovilli, C. Filippi, and F. M. Floris, J. Phys. Chem. B **110**, 26225 (2006).
[21] A. Bondi, J. Phys. Chem. **68**, 441 (1964).
[22] J. Tomasi and M. Persico, Chem. Rev. (Washington, D.C.) **94**, 2027 (1994).